Simulations of Li ion diffusion in the electrolyte material – Li_3PO_4 [a]

N. A. W. Holzwarth, Yaojun Du, and Xiao Xu
Wake Forest University, Winston-Salem, NC, USA

- Motivation
- Calculational methods
- Validation (Raman spectra)
- Diffusion in crystalline electrolyte
- Studies of "defect" structures
- Models of electrolyte-anode interfaces

[a] Supported by NSF DMR-0405456, 0427055, and 0705239.

Diagram of discharge operation for a Li-ion battery

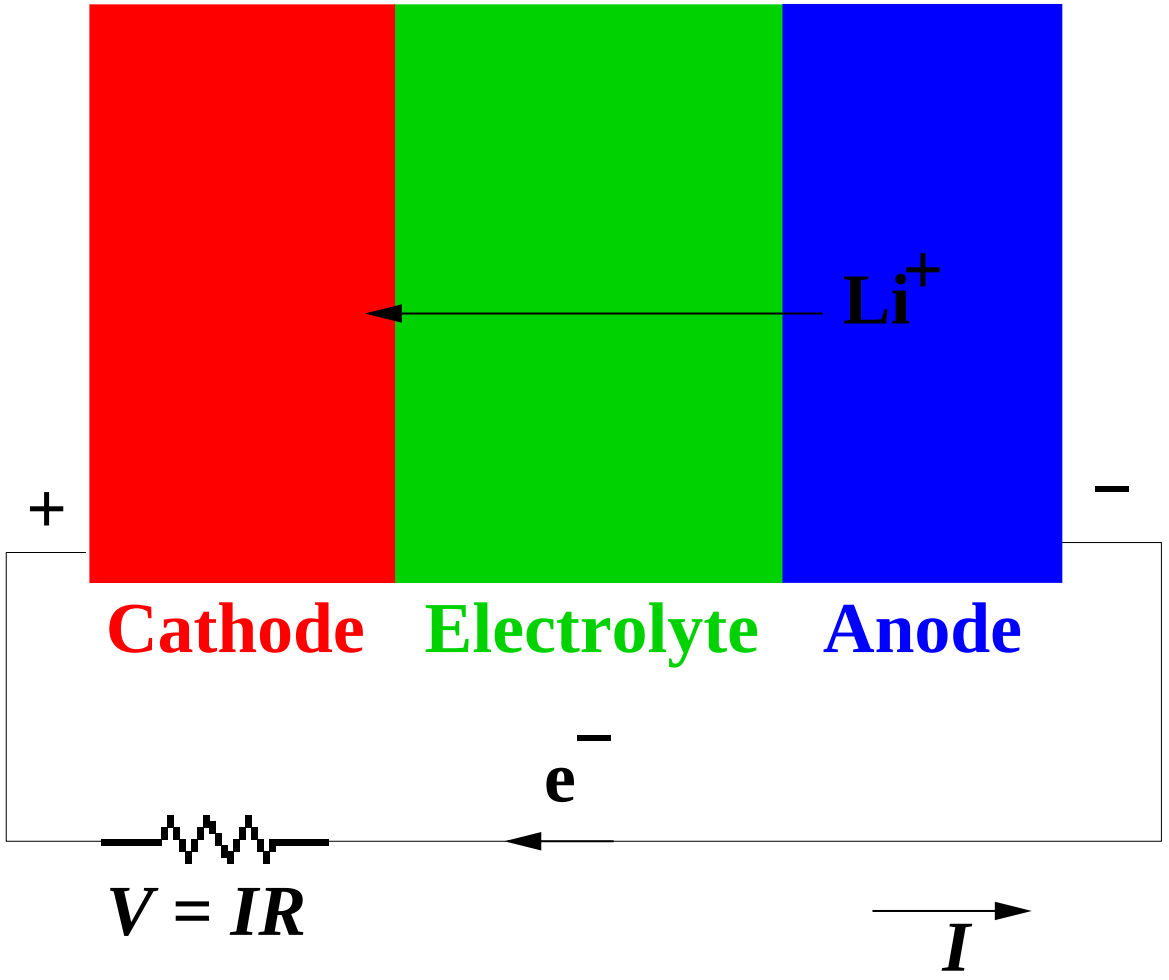

LiPON (Li_3PO_4 + N) developed at ORNL

Journal of Power Sources, 43–44 (1993) 103–110

Fabrication and characterization of amorphous lithium electrolyte thin films and rechargeable thin-film batteries

J. B. Bates, N. J. Dudney, G. R. Gruzalski, R. A. Zuhr, A. Choudhury and C. F. Luck
Oak Ridge National Laboratory, Oak Ridge, TN 37830 (USA)
J. D. Robertson
Department of Chemistry, University of Kentucky, Lexington, KY 40506 (USA)

Abstract

Amorphous oxide and oxynitride lithium electrolyte thin films were synthesized by r.f. magnetron sputtering of lithium silicates and lithium phosphates in Ar, $Ar+O_2$, $Ar+N_2$, or N_2. The composition, structure, and electrical properties of the films were characterized using ion and electron beam, X-ray, optical, photoelectron, and a.c. impedance techniques. For the lithium phosphosilicate films, lithium ion conductivities as high as 1.4×10^{-6} S/cm at 25 °C were observed, but none of these films selected for extended testing were stable in contact with lithium. On the other hand, a new thin-film lithium phosphorus oxynitride electrolyte, synthesized by sputtering Li_3PO_4 in pure N_2, was found to have a conductivity of 2×10^{-6} S/cm at 25 °C and excellent long-term stability in contact with lithium. Thin-films cells consisting of a 1 μm thick amorphous V_2O_5 cathode, a 1 μm thick oxynitride electrolyte film, and a 5 μm thick lithium anode were cycled between 3.7 and 1.5 V using discharge rates of up to 100 $\mu A/cm^2$ and charge rates of up to 20 $\mu A/cm^2$. The open-circuit voltage of 3.6 to 3.7 V of fully-charged cells remained virtually unchanged after months of storage.

Properties

- Chemical and structural stability.
- Reasonable Li^+ conductivity.
- Stable contacts with anodes and cathodes.

Questions

1. What are the basic mechanisms for Li^+ transport in crystalline Li_3PO_4?
   - Migration of Li^+ vacancies?
   - Migration of Li^+ interstitials?
2. What are the effects isolated defects in crystalline Li_3PO_4; competition between sources of mobile Li^+ ions and trapping effects. Neutral materials have the stoichiometries: $Li_{3+x}PO_{4-y}N_z$, with $x = 3z - 2y$.
   - Stable structures for isolated defects.
   - Effects of defects on Li^+ migration.
3. What happens at the interface between the electrolyte and electrode; ideal interfaces between crystalline Li_3PO_4 and metallic Li.
   - Plausible interface structures.
   - Migration of Li^+ vacancies or interstitials across interface.

Summary of "first-principles" calculational methods

Basic approximations

- All calculations are carried out using supercells composed of 16 Li_3PO_4 units.
- Nuclear motions are assumed to be separable from the electronic motions within the Born-Oppenheimer approximation and are treated classically.
- Electronic effects are treated within density functional theory (DFT) using the local density approximation (LDA) form of the exchange-correlation functional. (A few results were obtained using the generalized gradient approximation (GGA) form.) These calculations determine the "total energy" corresponding to the electronic ground state $E(\{\mathbf{R}^a\})$ and self-consistent electron density $\rho(\mathbf{r}, \{\mathbf{R}^a\})$ for each set of nuclear coordinates $\{\mathbf{R}^a\}$.
- Meta-stable configurations are determined by minimizing the total energies and converging the forces ($|\nabla_a E(\{\mathbf{R}^a\})| < 0.01$ eV/Å).
- Migration energies E_m between adjacent metal-stable configurations are determined using the Nudged Elastic Band method within an estimated error of ± 0.05 eV.

Codes for electronic structure calculations

Method	Comments
PAW *pwpaw* - `pwpaw.wfu.edu` *socorro* - `dft.sandia.gov/socorro` *abinit* - `www.abinit.org`	Works well for moderately large unit cells, but variable unit cell optimization not yet implemented in *pwpaw* and *socorro*. Need to construct and test PAW basis and projector functions.
LAPW *wien2k* - `www.wien2k.at`	Works well for smaller unit cells; variable unit cell optimization not implemented. Need to choose non-overlapping muffin tin radii and avoid "ghost" solutions.
PWscf *pwscf* - `www.pwscf.org`	Works well for large unit cells and includes variable unit cell optimization. Need to construct and test soft pseudopotential functions.

Secret recipe for pseudopotential construction

	r_c (bohr)	Atomic basis
Li		
PAW*	1.61	$1s, 2s, 2p$
PWscf†	1.60	$1s, 2s, 2p$
LAPW	1.70	$1s, \epsilon s, \epsilon p$
O		
PAW*	1.41	$2s, \epsilon s, 2p, \epsilon p$
PWscf†	1.40	$2s, \epsilon s, 2p, \epsilon p$
LAPW	1.28	$2s, \epsilon s, \epsilon p$
P		
PAW*	1.51	$2s, 3s, 2p, 3p$
PWscf†	1.50	$3s, \epsilon s, 3p, \epsilon p, \epsilon d$
LAPW	1.38	$\epsilon s, 2p, \epsilon p$

* PAW basis and projector functions generated by *atompaw* code.

† Ultra-soft pseudopotentials generated by *uspp* code of David Vanderbilt.

Test results for simple oxides

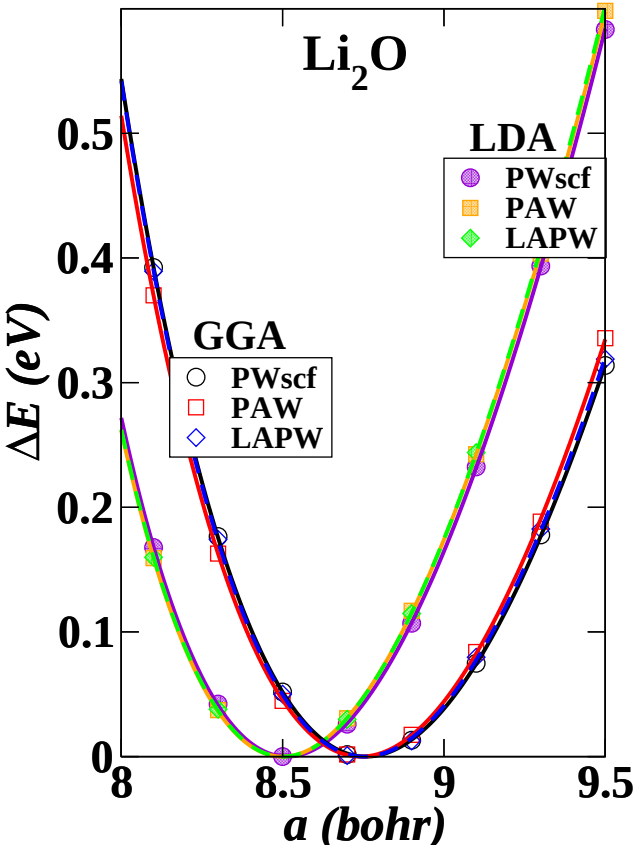

Fluorite structure

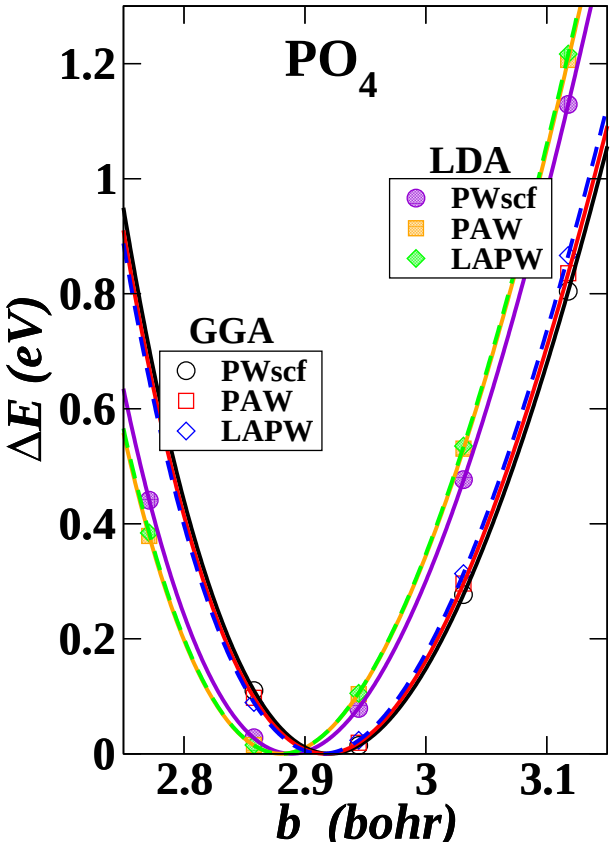

Tetrahedral molecule

Validation of calculations – comparison with Raman spectral data

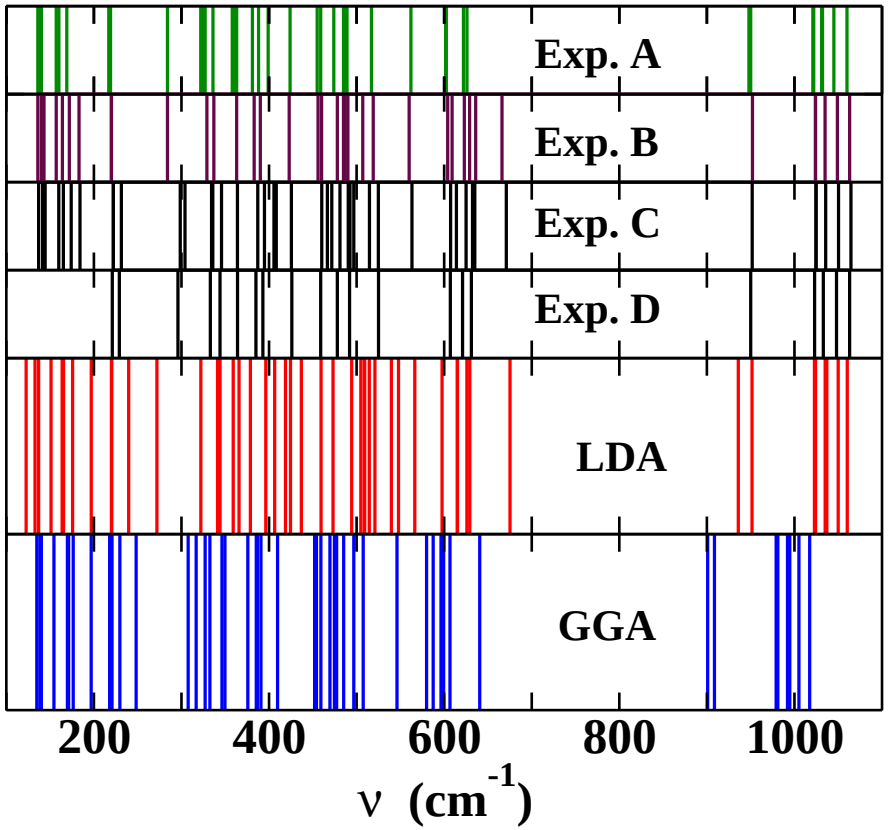

γ-Li_3PO_4

Exp. A – (RT) – Mavrin & co-workers, *JETP* **96**, 53 (2003); Exp. B – (RT) – Harbach & co-workers, *Phys. Stat. Sol. B* **66**, 237 (1974); Exp. C – (LNT) – Harbach; Exp. D – (LNT) Popović & co-workers, *J. Raman Spec.* **34** 77, (2003)

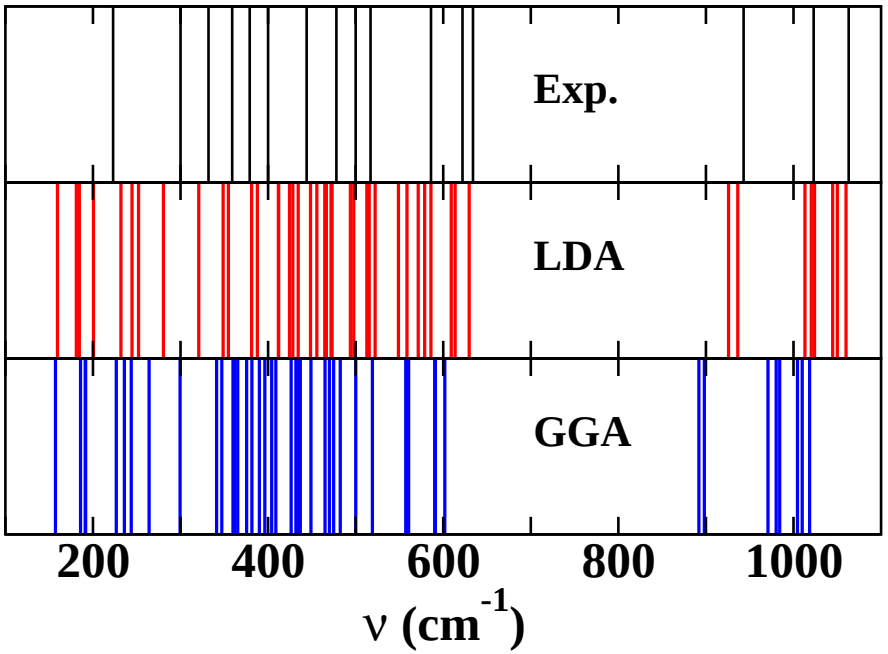

β-Li_3PO_4

Exp. – (LNT) Popović & co-workers, *J. Raman Spec.* **34** 77, (2003)

Ionic conductivity via activated hopping

Schematic diagram of minimal energy path

Approximated using NEB algorithm[a]
– "Nudged Elastic Band"

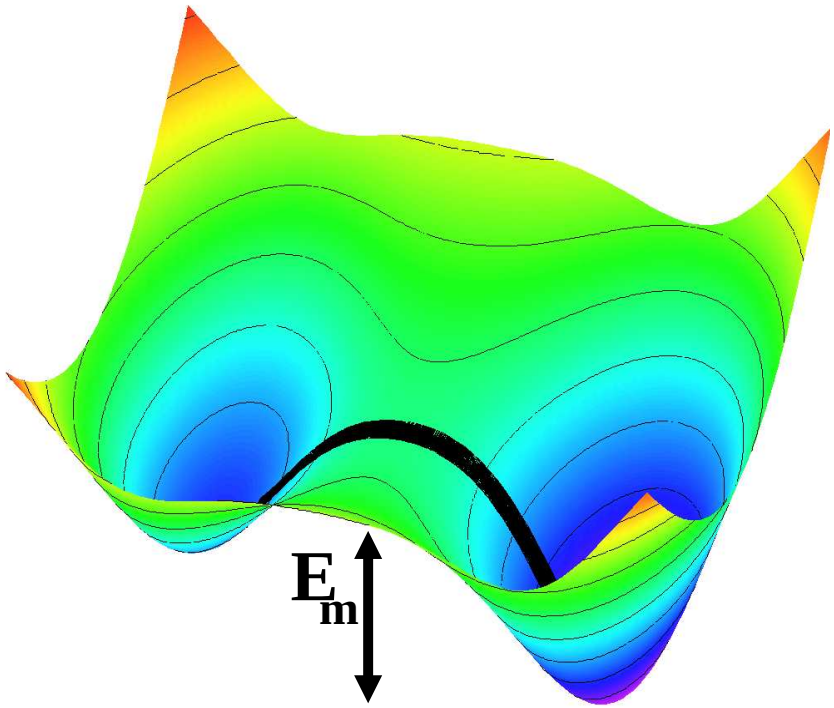

[a]H. Jónsson et al., in *Classical and Quantum Dynamics in Condensed Phase Simulations*, edited by Berne, Ciccotti, and Coker (World Scientific, 1998), p. 385; G. Henkelman et al, *JCP* **113**, 9901, 9978 (2000).

Arrhenius relation

$$\sigma \cdot T = K \mathrm{e}^{-E_A/kT}$$

From: Ivanov-Shitz and co-workers, *Cryst. Reports* **46**, 864 (2001):

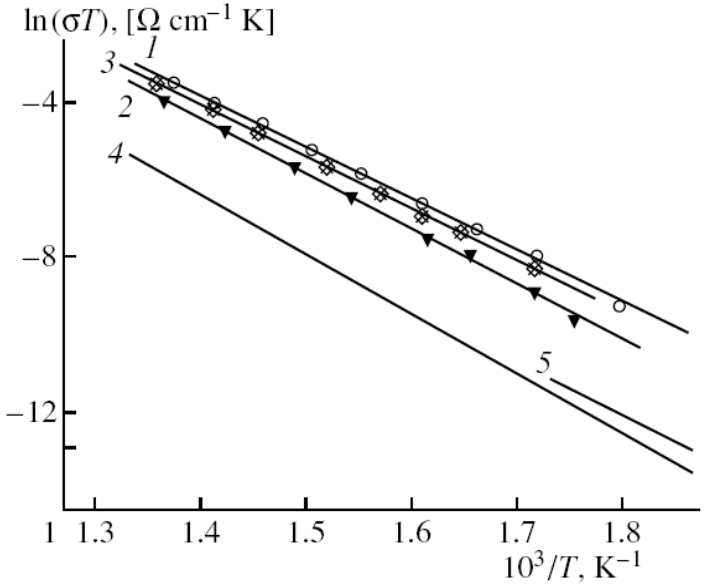

Fig. 2. Temperature dependences of conductivity in γ-Li_3PO_4: (*1–3*) for single crystals measured along the (*1*) *a*-axis, (*2*) *b*-axis, (*3*) *c*-axis and (*4, 5*) for a polycrystal (*4*) according to [4, 5] and (*5*) according to [7].

E_A = 1.14, 1.23, 1.14, 1.31, 1.24 eV for 1,2,3,4,5, respectively.

Crystalline Li_3PO_4

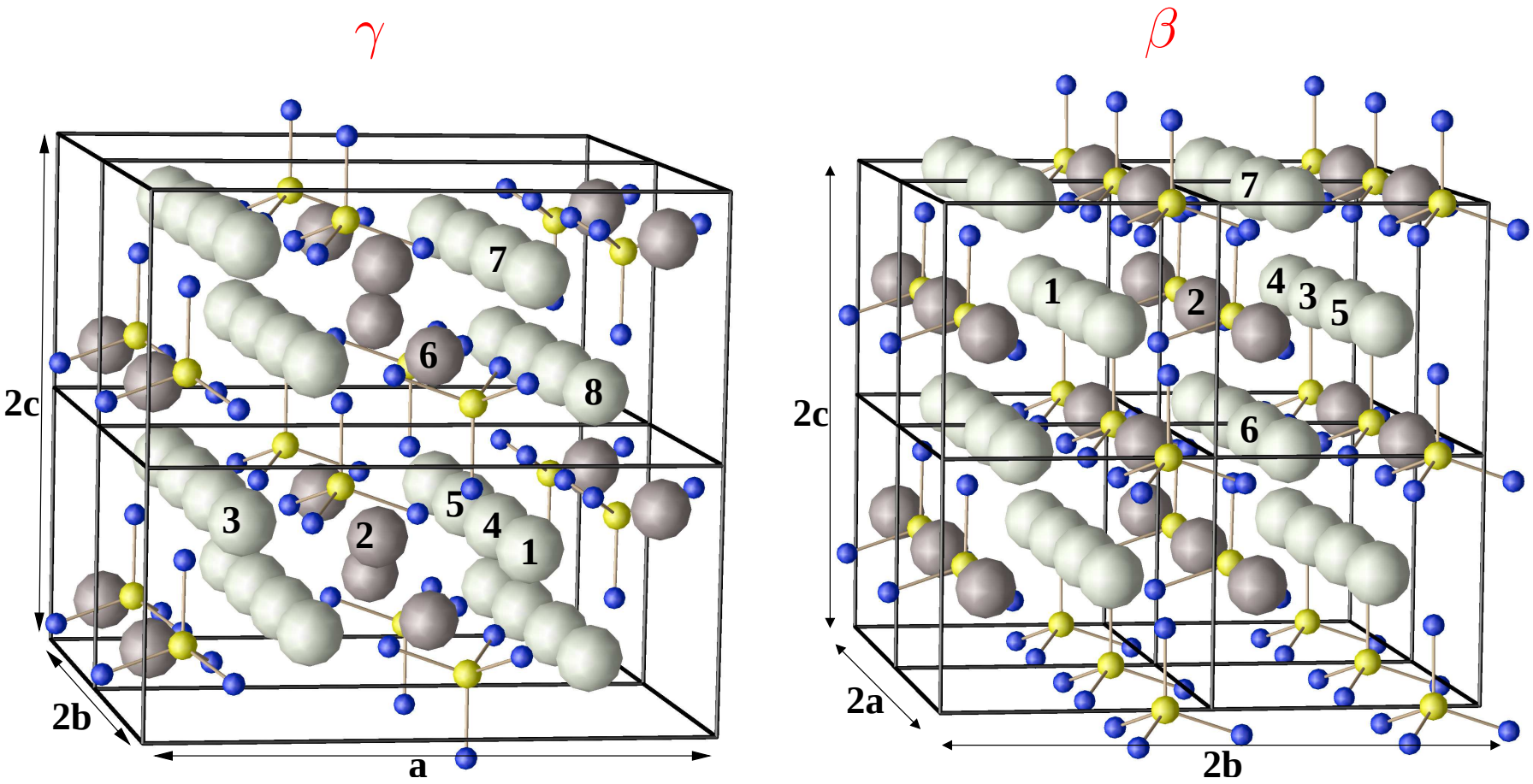

Ball and stick drawing of the equilibrium structures of the γ-Li_3PO_4 and β-Li_3PO_4 supercells used in the simulations. The PO_4 groups are indicated with bonded yellow and blue spheres. Li ions are indicated by light and dark gray spheres representing the crystallographically distinct sites. The number labels on some of the Li sites are used to describe vacancy diffusion.

Example of configuration coordinate diagrams for vacancy diffusion in Li_3PO_4

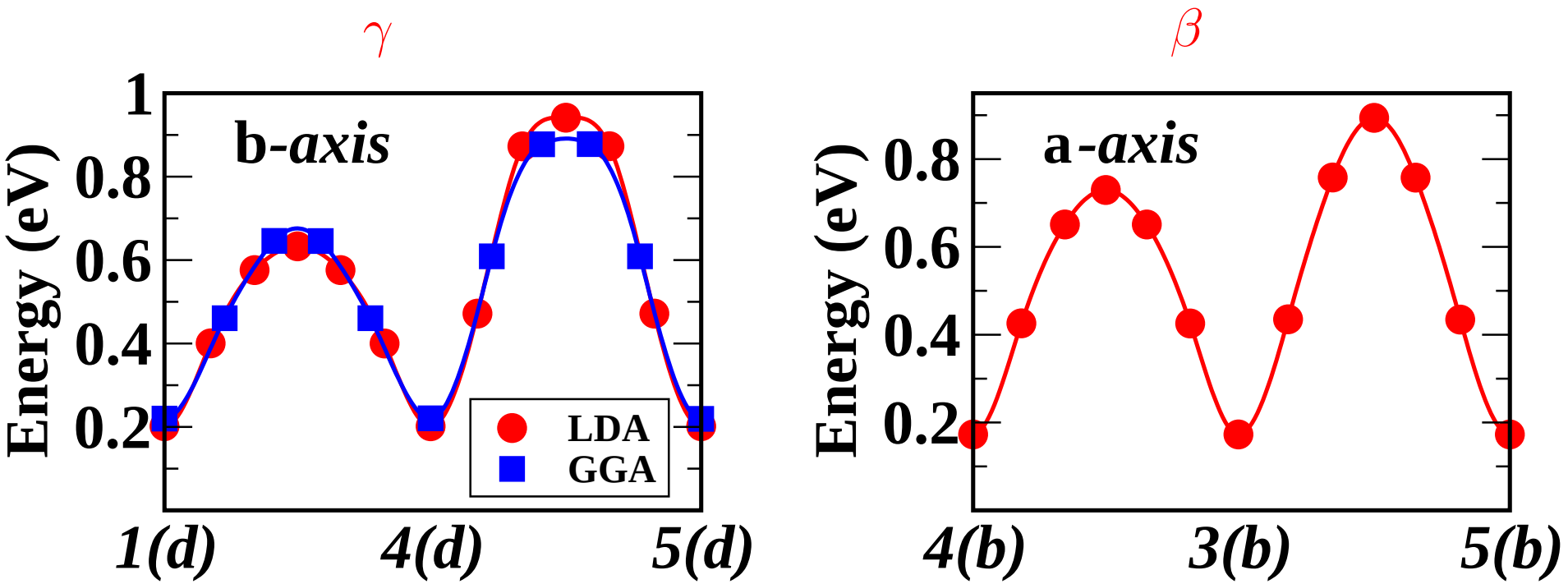

Metastable interstitial Li^+ configurations in γ-Li_3PO_4

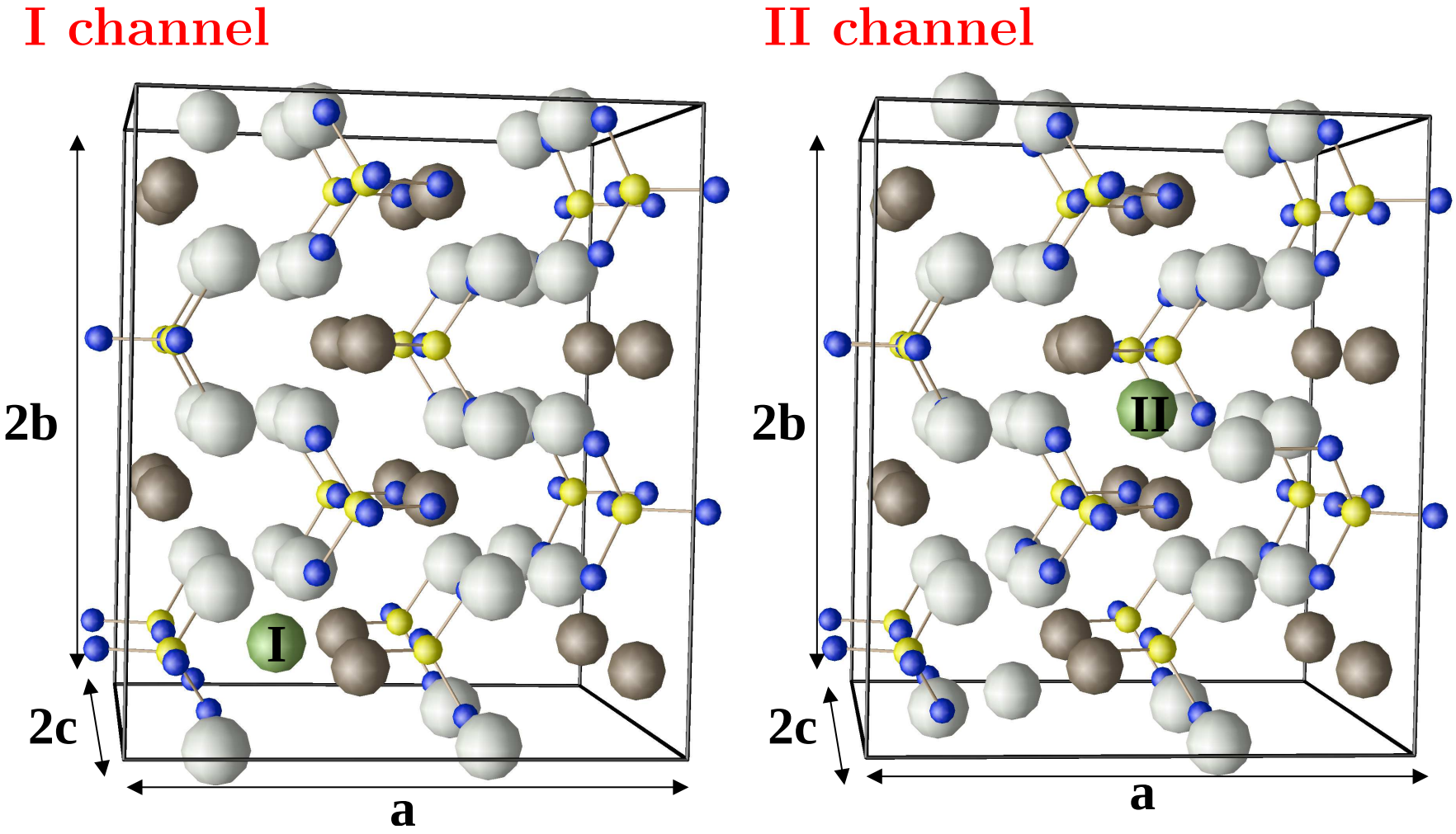

Ball and stick drawing of the metastable interstitial Li^+ sites (indicated with green balls) in γ-Li_3PO_4. Similar structures occur in β-Li_3PO_4.

Example of configuration coordinate diagrams for interstitial diffusion in Li_3PO_4

γ

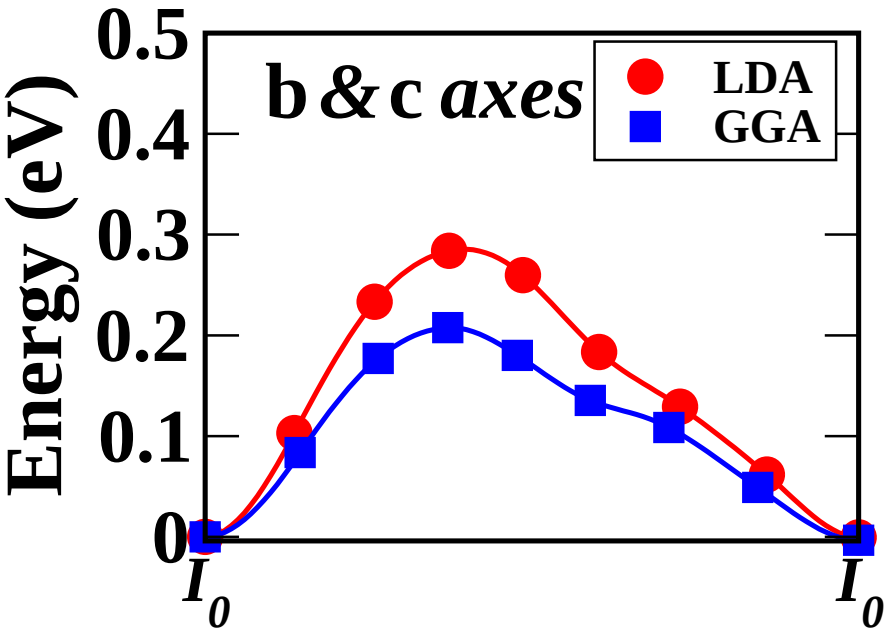

β

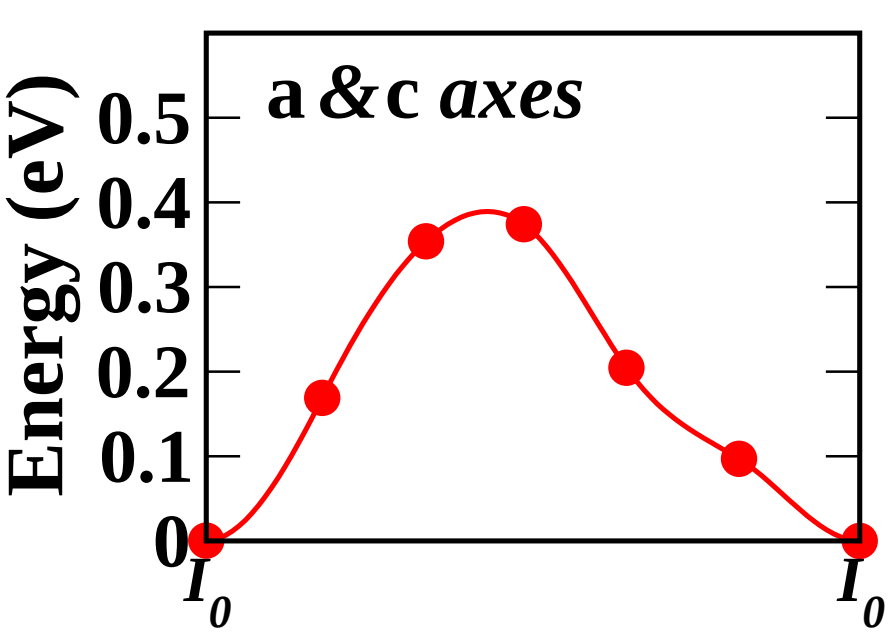

Illustration of interstitialcy mechanism along b & c axes in γ-Li_3PO_4

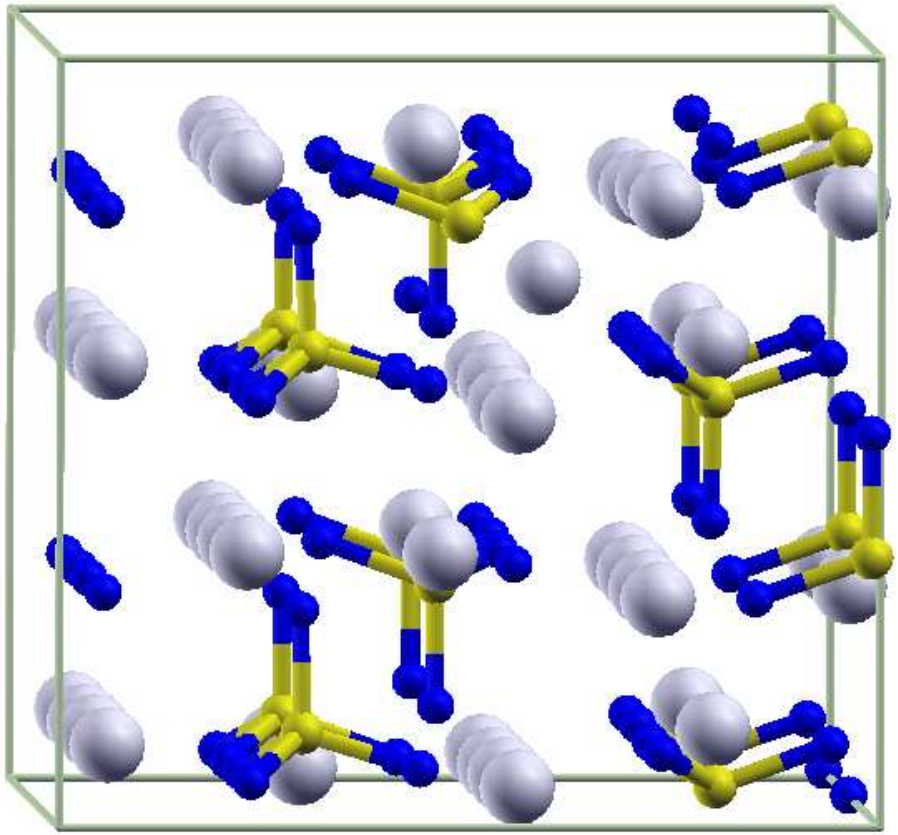

Illustration of interstitialcy mechanism along b & c axes in γ-Li_3PO_4

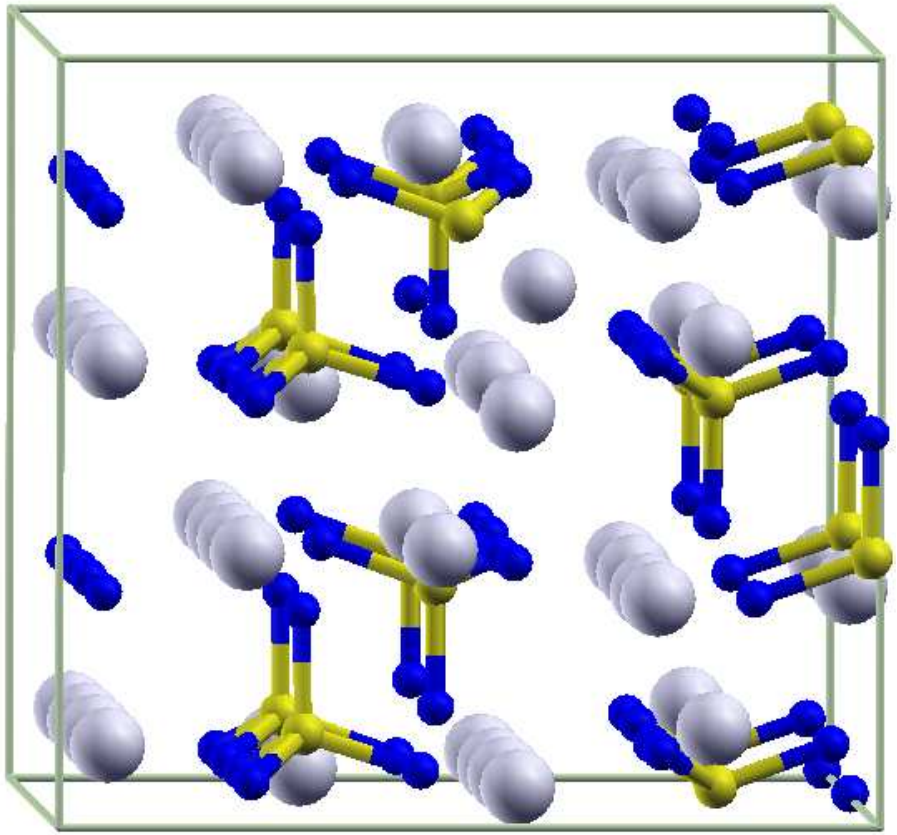

Illustration of interstitialcy mechanism along b & c axes in γ-Li_3PO_4

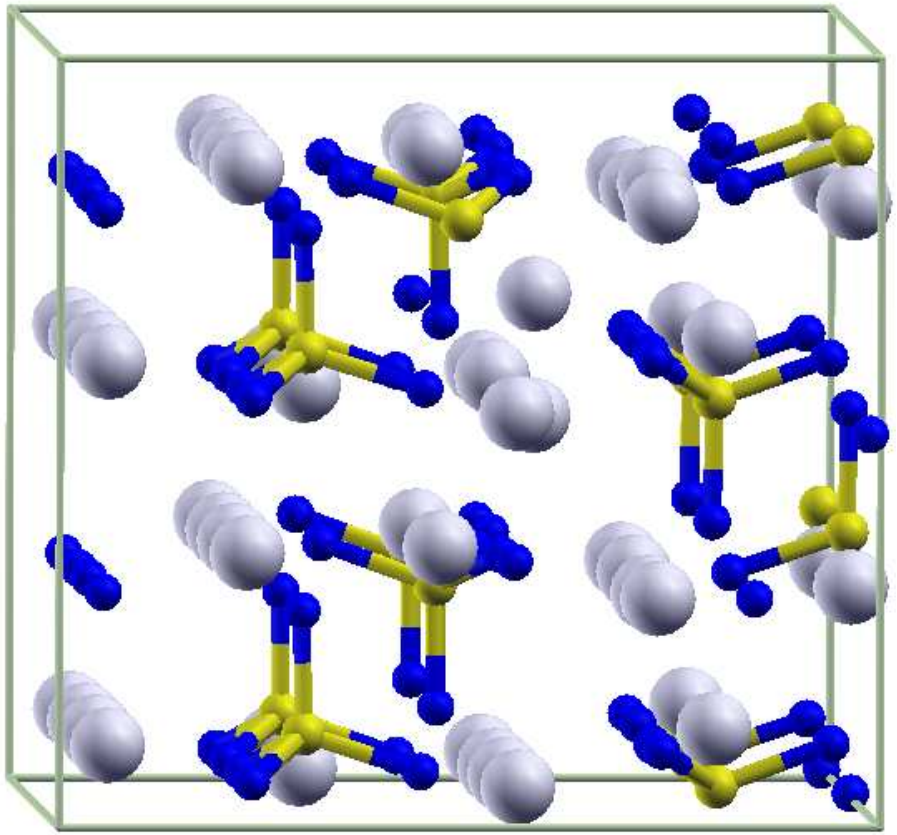

Illustration of interstitialcy mechanism along b & c axes in γ-Li_3PO_4

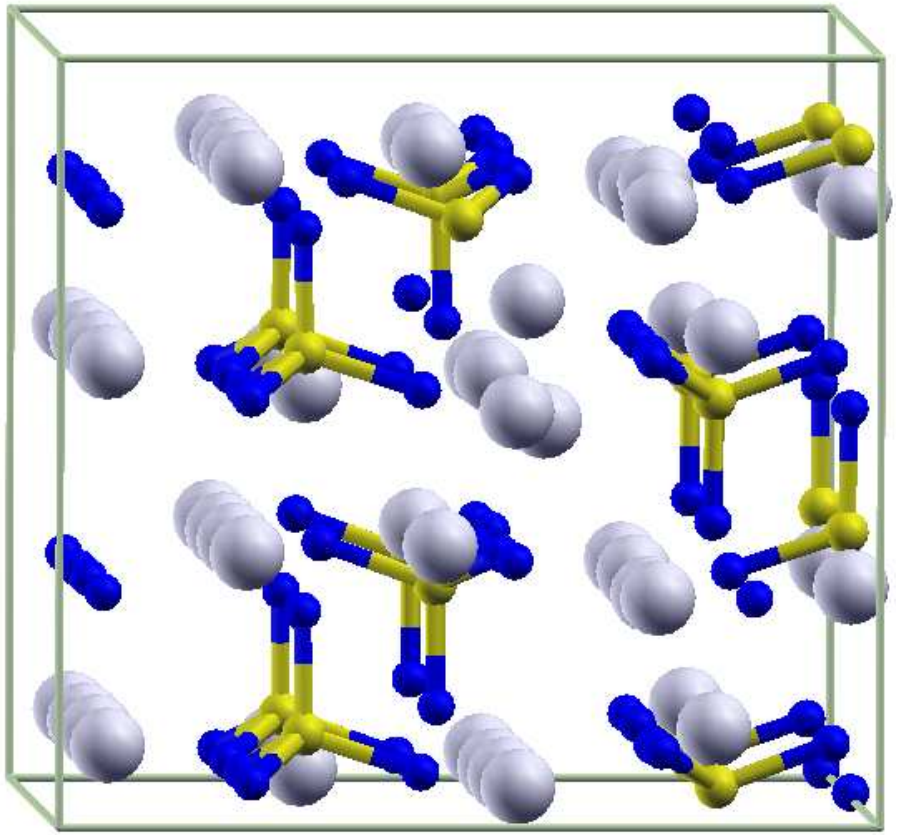

Illustration of interstitialcy mechanism along b & c axes in γ-Li_3PO_4

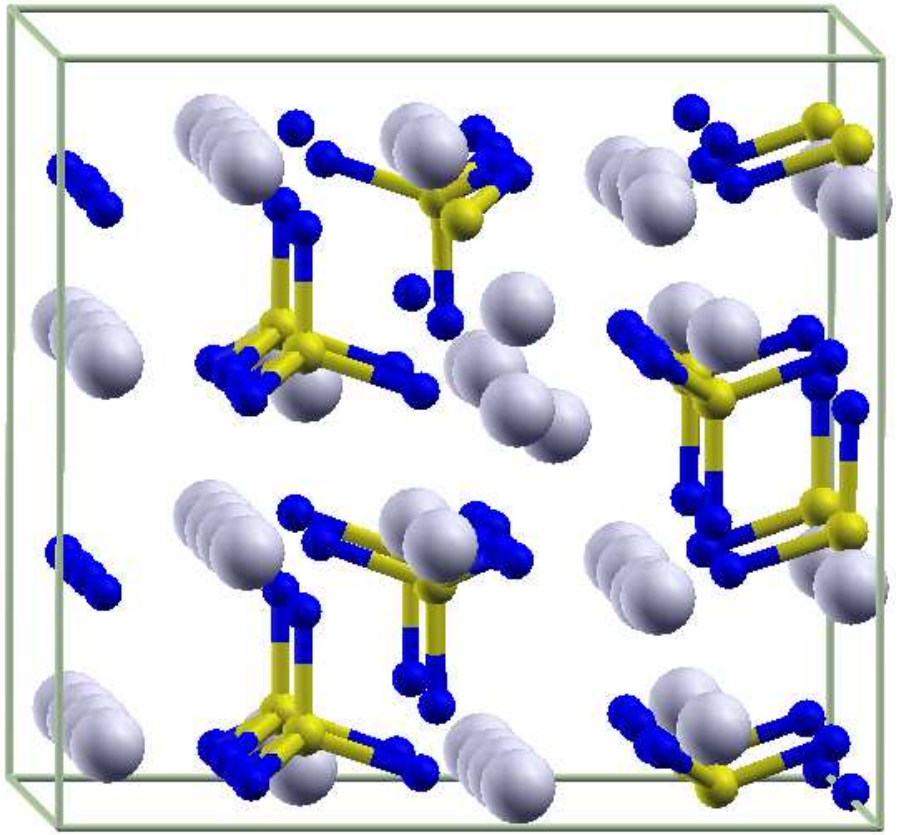

Illustration of interstitialcy mechanism along b & c axes in γ-Li_3PO_4

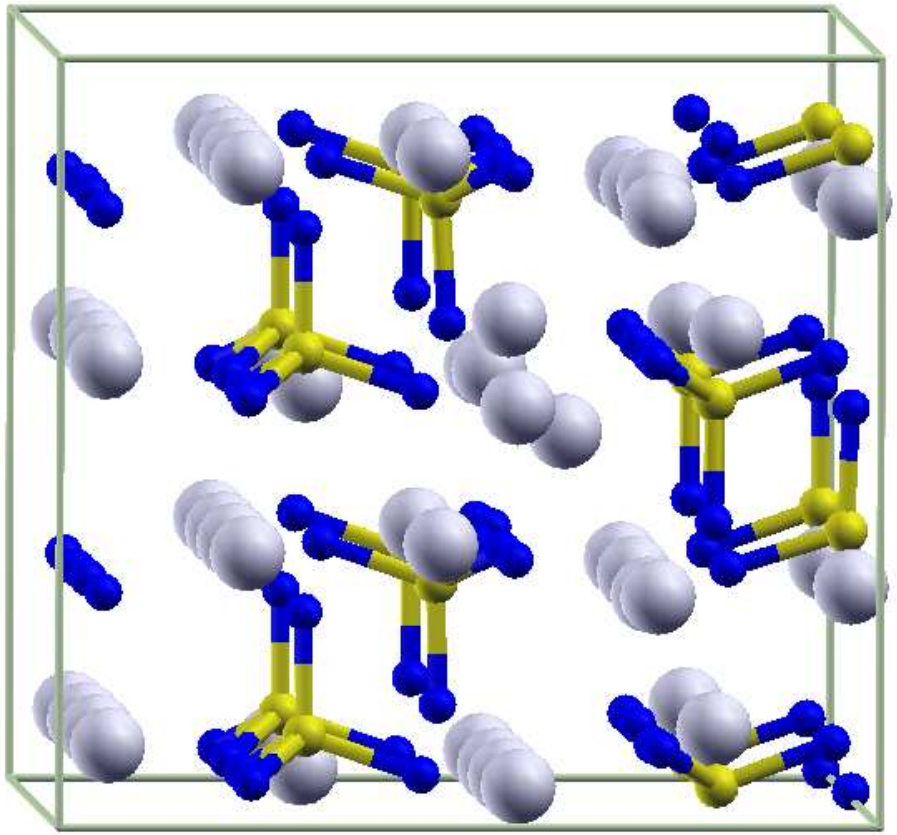

Illustration of interstitialcy mechanism along b & c axes in γ-Li_3PO_4

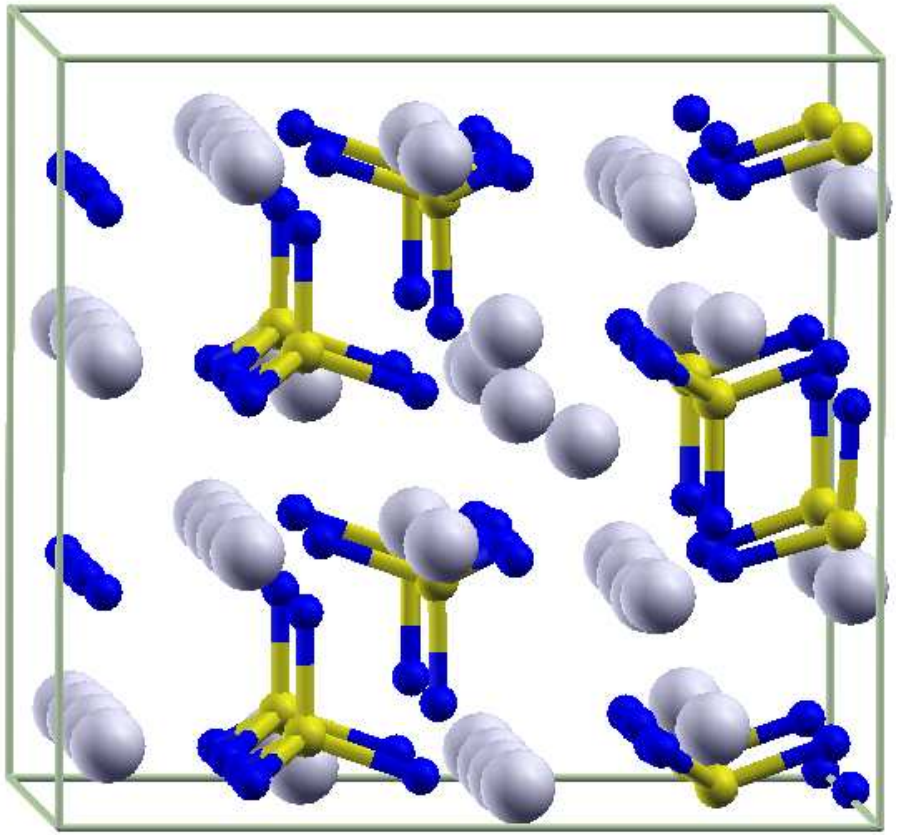

Illustration of interstitialcy mechanism along b & c axes in γ-Li_3PO_4

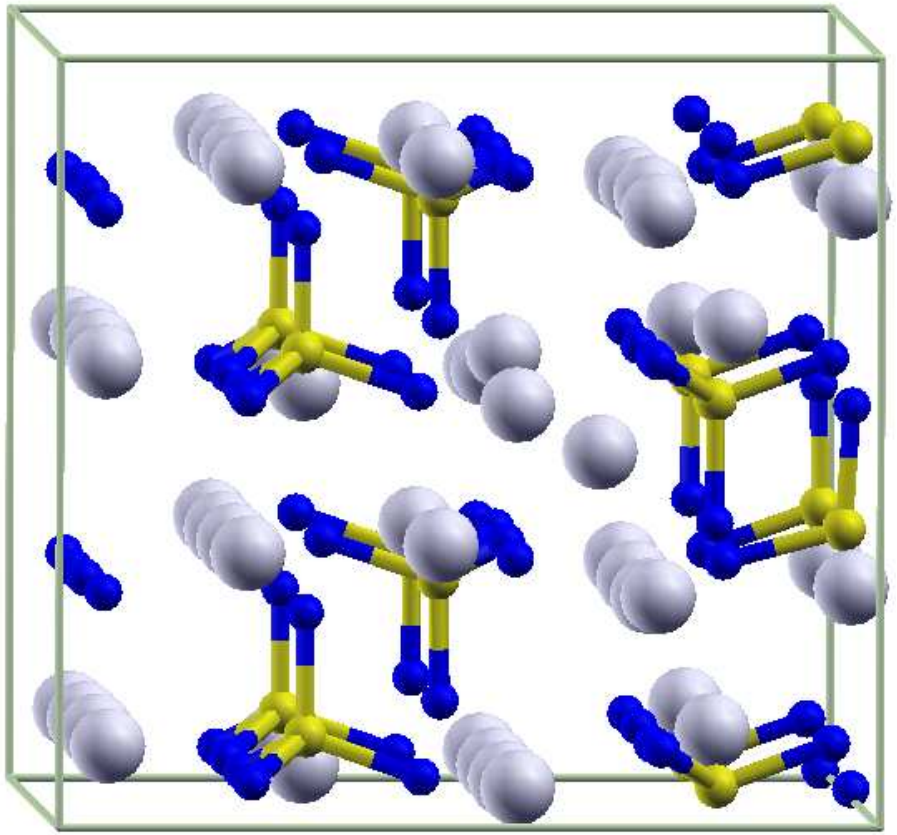

Illustration of interstitialcy mechanism along b & c axes in γ-Li_3PO_4

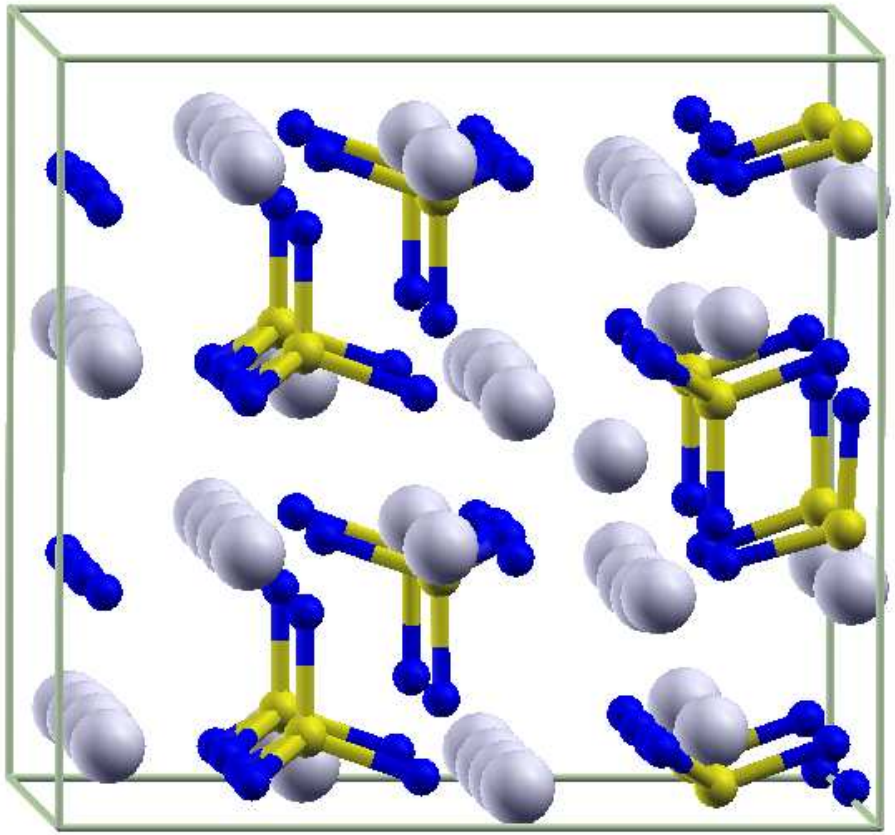

Li^+ ion energies in bulk γ-Li_3PO_4 crystals[a]

Axis	E_m	$E_A = E_m + E_f/2$[b]	E_A (exp)[c]
a (vacancy)	0.7 eV	1.5 eV	
a (interstitial)	0.4 eV	1.3 eV	1.23 eV
b (vacancy)	0.7 eV	1.5 eV	
b (interstitial)	0.3 eV	1.1 eV	1.14 eV
c (vacancy)	0.7 eV	1.5 eV	
c (interstitial)	0.3 eV	1.1 eV	1.14 eV

[a] Yaojun Du and N. A. W. Holzwarth, *PRB* **76**, 174302 (2007).

[b] $E_f \approx 1.7$ eV.

[c] Ivanov-Shitz et al, *Cryst. Reports* **46**, 864 (2001).

Defect structures – γ-$Li_{3-\frac{1}{16}}PO_{4-\frac{2}{16}}N_{\frac{1}{16}}$

Stable "bent" P–N–P structure

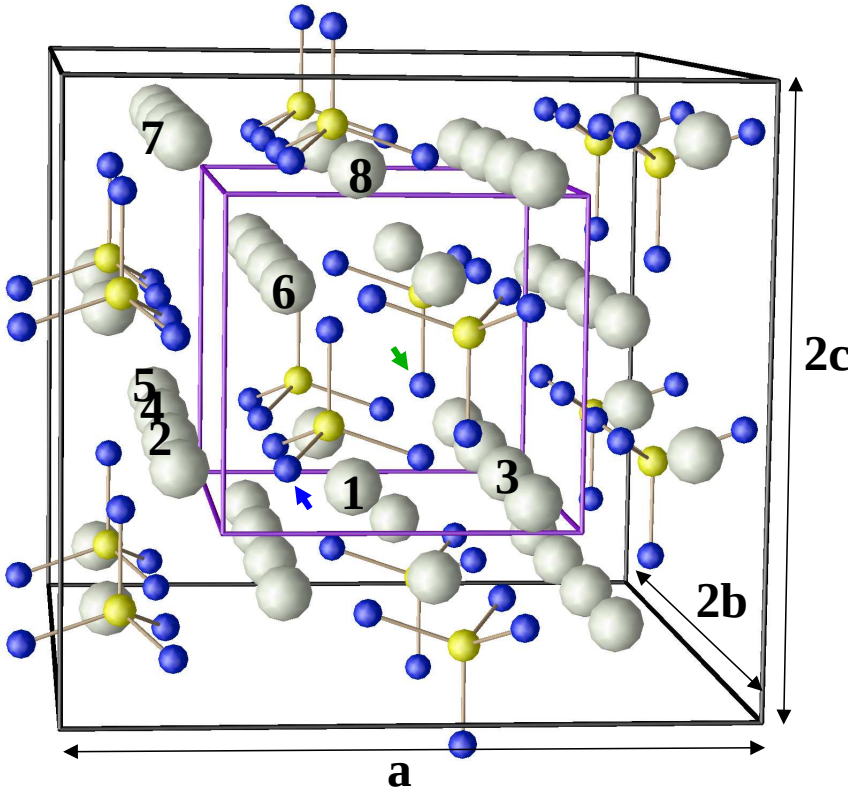

Ideal supercell

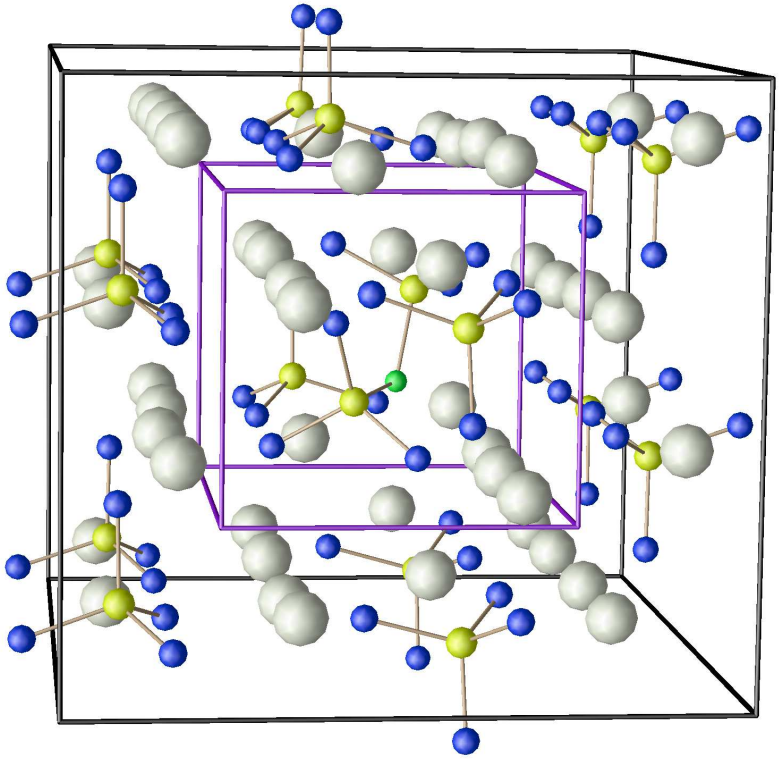

Relaxed structure

Defect structures – γ-$Li_{3-\frac{1}{16}}PO_{4-\frac{2}{16}}N_{\frac{1}{16}}$

Stable "bent" P–N–P and P–O–P structures

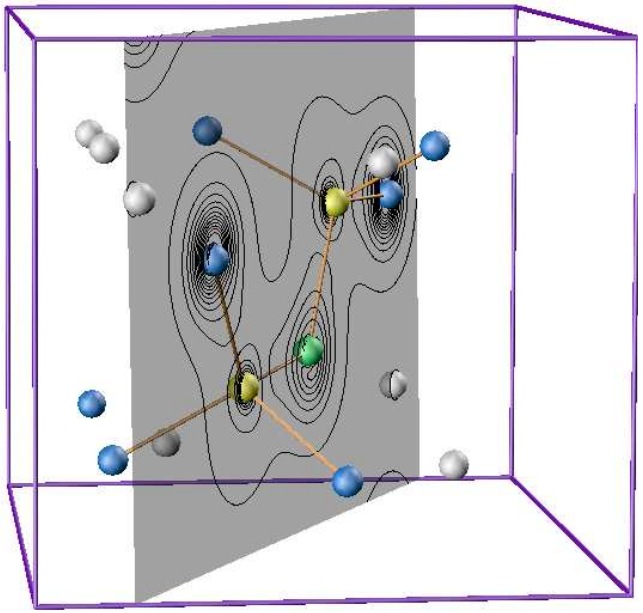

Contours of electron density for "bent" P–N–P structure

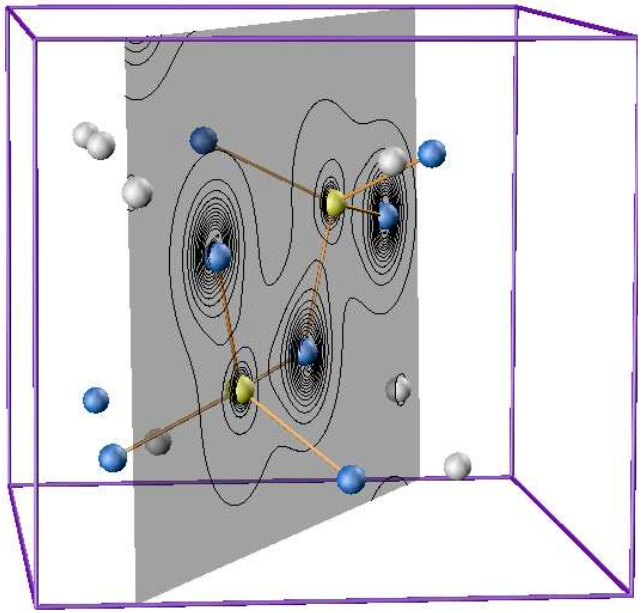

Contours of electron density for "bent" P–O–P structure

Defect structures – γ-$Li_{3-\frac{1}{16}}PO_{4-\frac{2}{16}}N_{\frac{1}{16}}$

Stable "straight" P–N–P structure

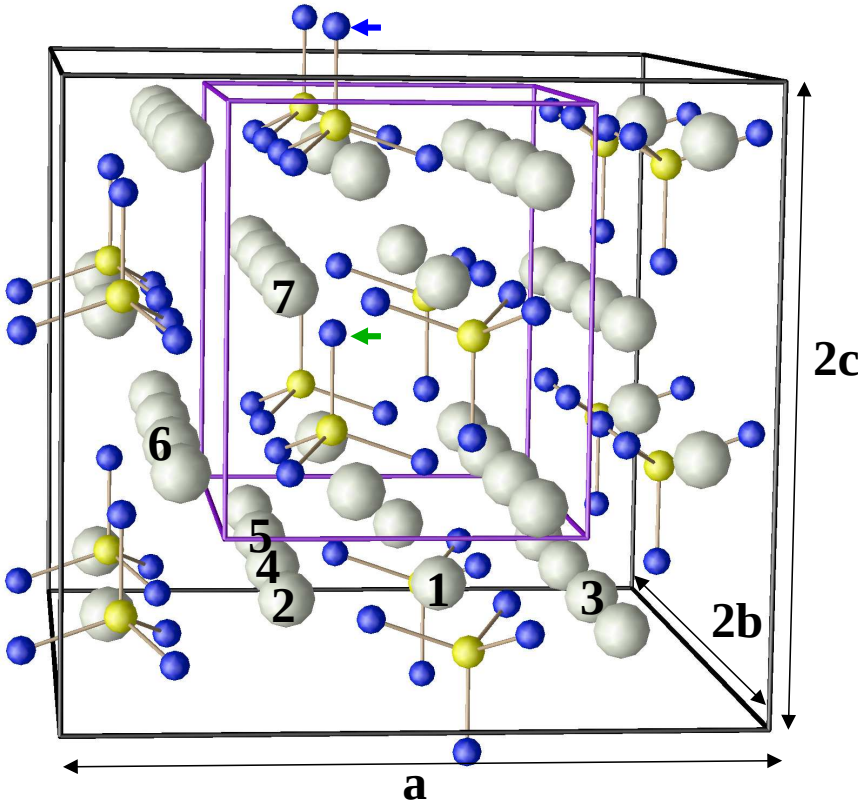

Ideal supercell

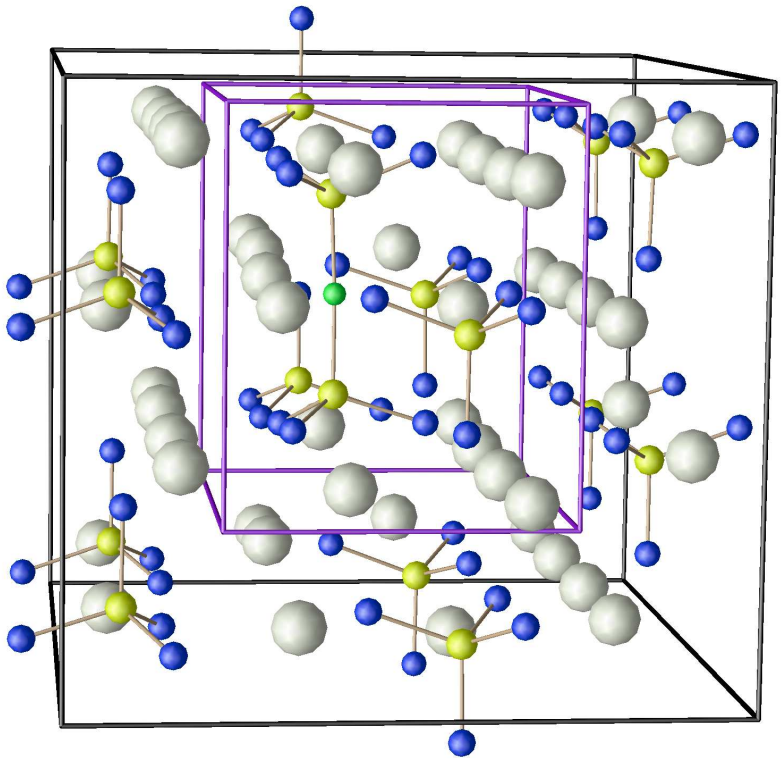

Relaxed structure

Defect structures – γ-$Li_{3-\frac{1}{16}}PO_{4-\frac{2}{16}}N_{\frac{1}{16}}$

Stable "straight" P–N–P and P–O–P structures

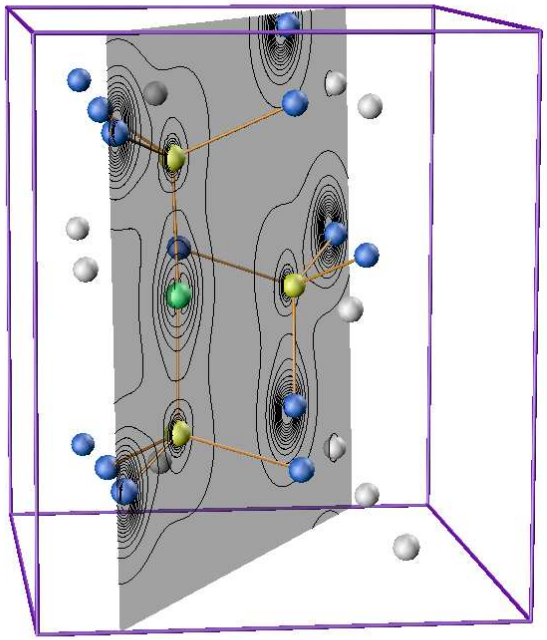

Contours of electron density for "straight" P–N–P structure

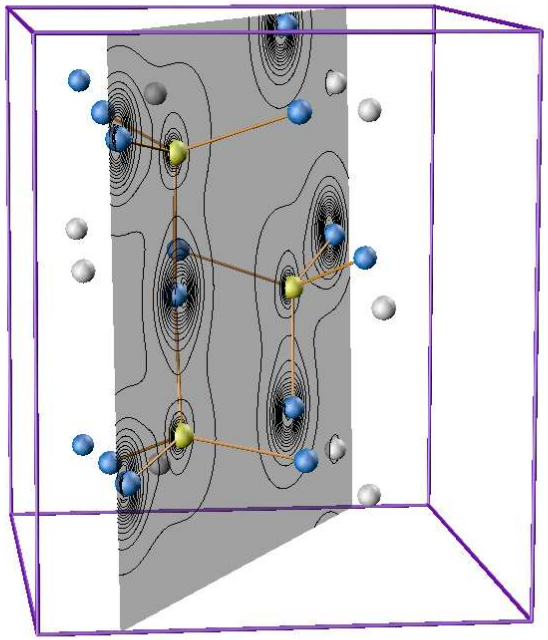

Contours of electron density for "straight" P–O–P structure

Summary of properties of defect structures in γ-Li_3PO_4.

Bond lengths, angles, and relative supercell energies for P−N−P and P−O−P structures.

Type	Bond lengths (Å)*	Bond angle	Energy (eV)
P−N−P (bent)	1.63, 1.66	118(°)	0.00
P−N−P (straight)	1.63, 1.62	174(°)	0.05
P−O−P (bent)	1.66, 1.70	122(°)	2.71
P−O−P (straight)	1.69, 1.66	171(°)	2.59

* For comparison, tetrahedral P−O bonds are calculated to be 1.54-1.57 Å.

Effects of PNP structures on Li^+ vacancy migration energies

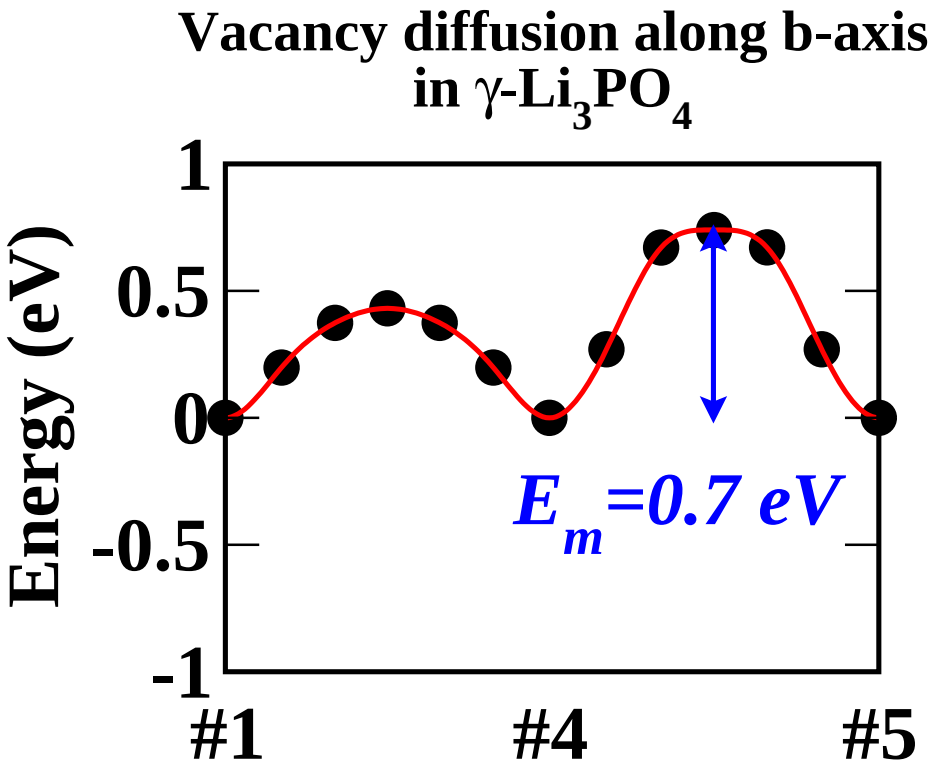

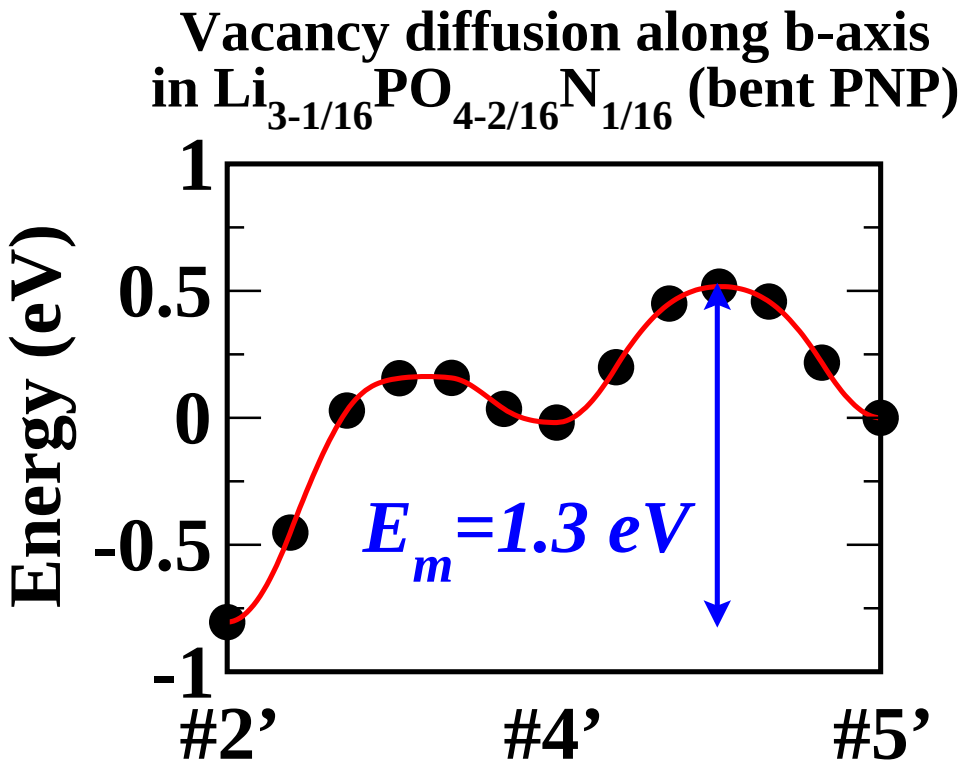

Li^+ ion energies in dopped γ-Li_3PO_4 crystals

Axis	E_m (perfect crystal)[a]	E_m (dopped crystal)
a (vacancy)	0.7 eV	0.8 eV[b]
a (interstitial)	0.4 eV	
b (vacancy)	0.7 eV	1.3 eV[b]
b (interstitial)	0.3 eV	0.7-0.9 eV[c]
c (vacancy)	0.7 eV	0.9 eV[b]
c (interstitial)	0.3 eV	0.7-0.9 eV[c]

[a] Yaojun Du and N. A. W. Holzwarth, *PRB* **76**, 174302 (2007).

[b] $Li_{3-1/16}PO_{4-2/16}N_{1/16}$ in bent PNP structure.

[c] $Li_{3+1/16}PO_{4-1/16}N_{1/16}$ for various N substitution positions.

$\Rightarrow$ Isolated defects trap Li^+ ions.

Interfaces between Li_3PO_4 and Li metal

Normal axis	Simulation supercell geometry	Diffusion mechanism
a-axis:	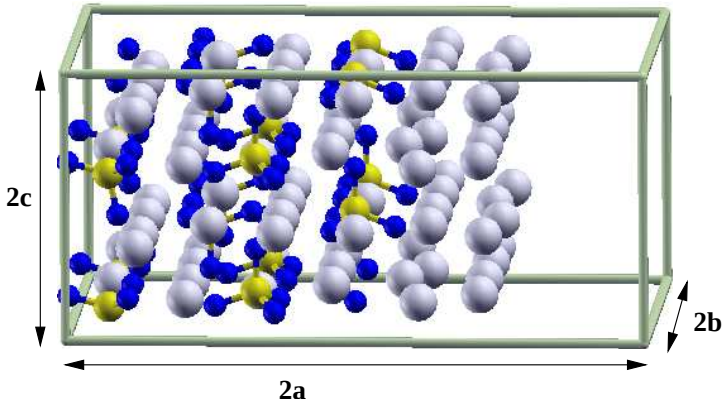	vacancy
b-axis:	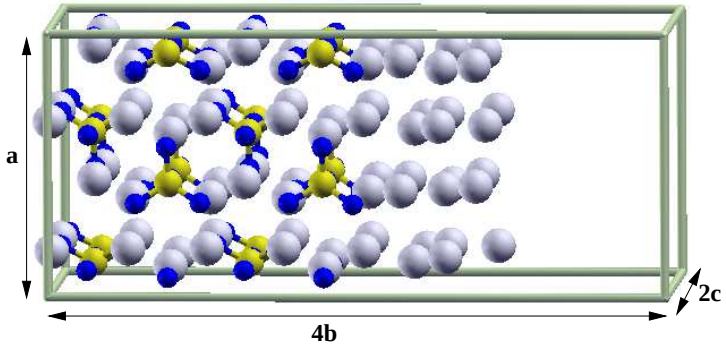	interstitial
c-axis:	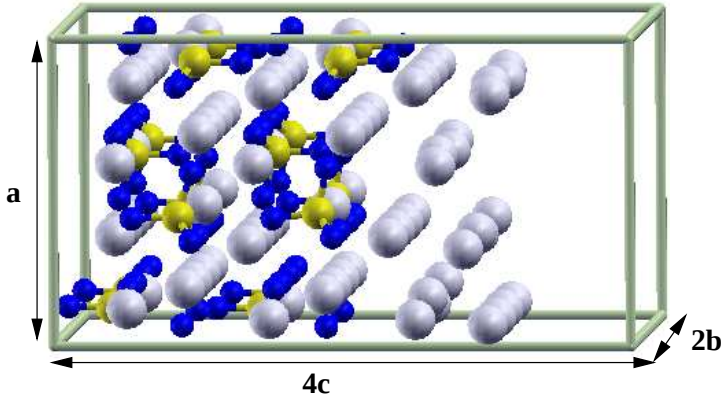	interstitial

Partial densities of states interfaces (along a-axis)

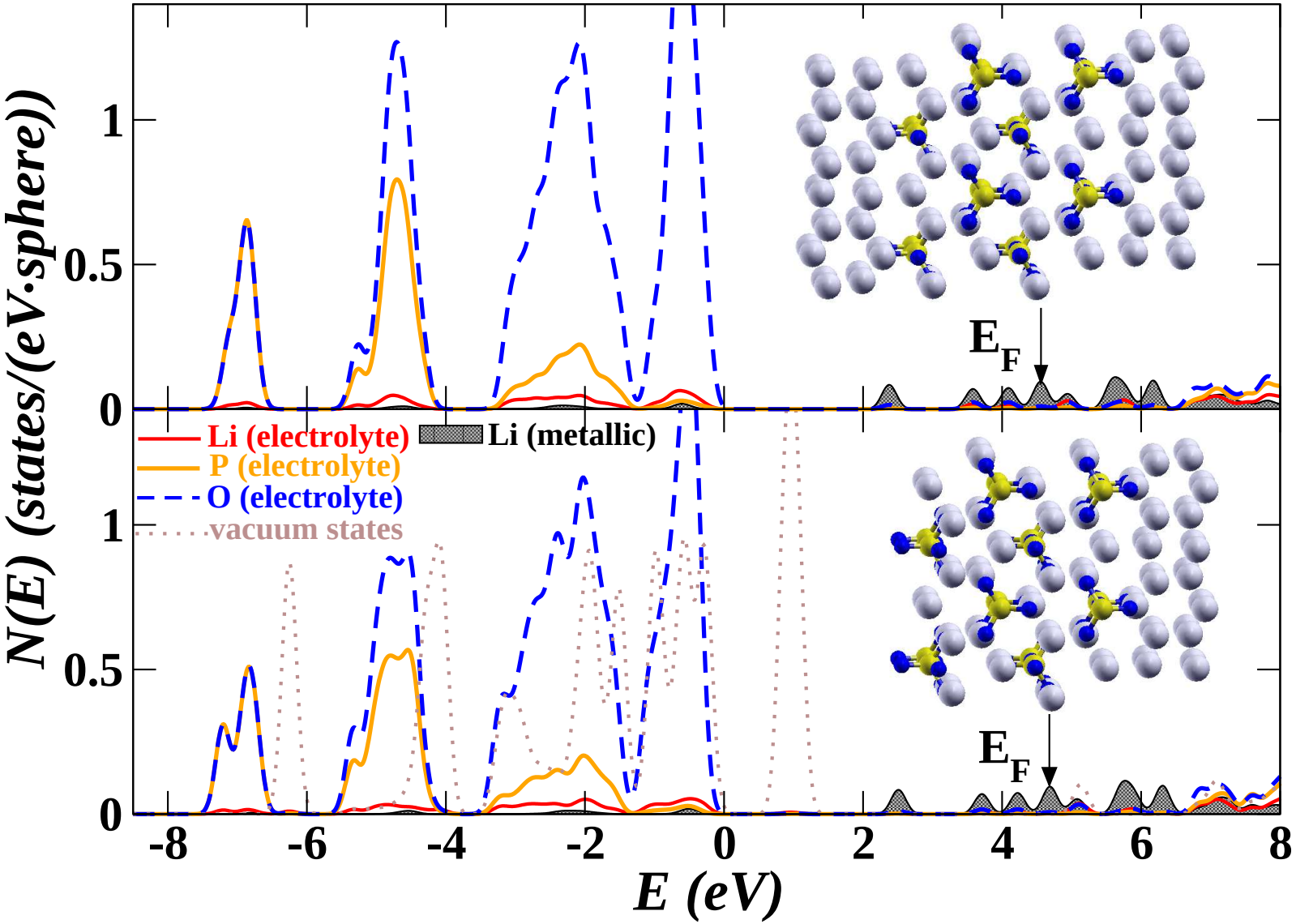

Vacancy diffusion across interface in a-direction via direct hopping mechanism

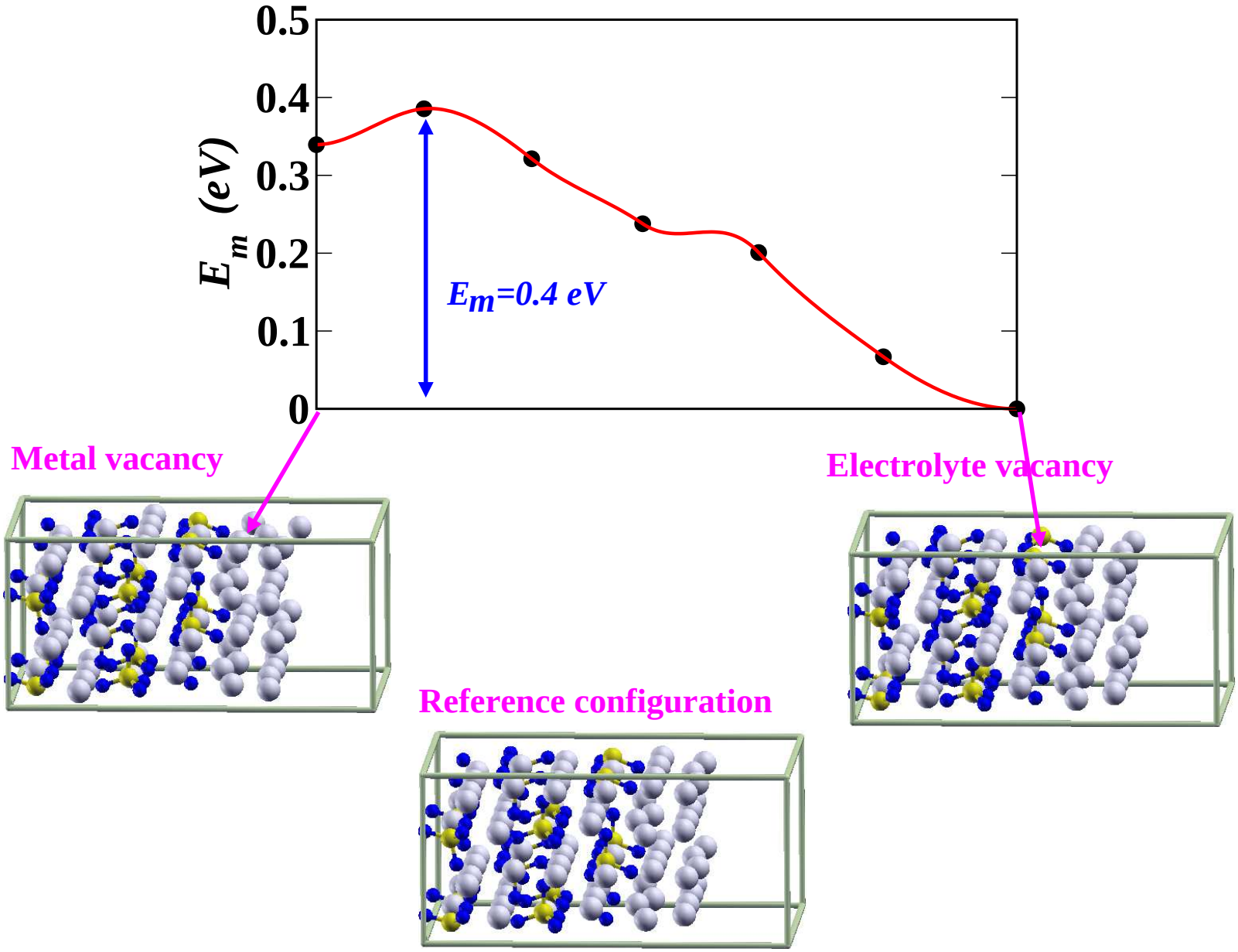

Comparison of Li ion migration energies for bulk and interface diffusion in γ-Li_3PO_4

Axis	E_m (bulk crystal)[a]	E_m (interface)
a (vacancy)	0.7 eV	0.4 eV
a (interstitial)	0.4 eV	??
b (vacancy)	0.7 eV	0.2 eV
b (interstitial)	0.3 eV	0.2-0.3 eV
c (vacancy)	0.7 eV	??
c (interstitial)	0.3 eV	0.3 eV

[a] Yaojun Du and N. A. W. Holzwarth, *PRB* **76**, 174302 (2007).

$\Rightarrow$ E_m**(interface)** $\leq$ E_m**(bulk).**

Questions

1. What are the basic mechanisms for Li^+ transport in crystalline Li_3PO_4?
   - Migration of Li^+ vacancies?
   - Migration of Li^+ interstitials?
2. What are the effects isolated defects in crystalline Li_3PO_4; competition between sources of mobile Li^+ ions and trapping effects. Neutral materials have the stoichiometries: $Li_{3+x}PO_{4-y}N_z$, with $x = 3z - 2y$.
   - Stable structures for isolated defects.
   - Effects of defects on Li^+ migration.
3. What happens at the interface between the electrolyte and electrode; ideal interfaces between crystalline Li_3PO_4 and metallic Li.
   - Plausible interface structures.
   - Migration of Li^+ vacancies or interstitials across interface.

Some Answers

1. What are the basic mechanisms for Li^+ transport in crystalline Li_3PO_4?
   - Migration of Li^+ vacancies? $E_m \approx 0.6 - 0.7$ eV.
   - Migration of Li^+ interstitials? $E_m \approx 0.3 - 0.5$ eV.
   - Good agreement with activation energy measurements on γ-Li_3PO_4 $E_A = E_m + E_f/2 \approx 1.1 - 1.3$ eV.

2. What are the effects isolated defects in crystalline Li_3PO_4; competition between sources of mobile Li^+ ions and trapping effects. Neutral materials have the stoichiometries: $Li_{3+x}PO_{4-y}N_z$, with $x = 3z - 2y$.
   - Stable structures for isolated defects; for $z = 2y = -x = 1/16$ find rebonded P−N−P and P−O−P structures. Also studied $z = y = x = 1/16$.
   - Effects of defects on Li^+ migration – Isolated defects within crystalline Li_3PO_4 tend to trap Li^+ ions and increase their migration energies.

3. What happens at the interface between the electrolyte and electrode; ideal interfaces between crystalline Li_3PO_4 and metallic Li.
   - Plausible interface structures – idealized model interfaces along a, b, and c axes are found to be physically and chemically stable.
   - Migration of Li^+ vacancies or interstitials across interface. Find $E_m(\text{interface}) \leq E_m(\text{bulk})$.